Microalloyed Niobium Steel

Subjects: Ergonomics

Contributor: Ljerka Slokar BeniÄ

Thermomechanical processing of niobium microalloyed steel was performed with the purpose of determining the interaction between niobium precipitates and dislocations, as well as determining the influence of the temperature of final deformation on the degree of precipitation and dislocation density. Two variants of thermomechanical processing with dierent final rolling temperatures were carried out. Samples were studied using electrochemical isolation with an atomic absorption spectrometer, transmission electron microscopy, X-ray diraction analysis, and universal tensile testing with a thermographic camera. The results show that the increase in the density of dislocations before the onset of intense precipitation is insignificant because the recrystallization process takes place simultaneously. It increases with the onset of strain-induced precipitation. It is shown that niobium precipitates determine the density of dislocations. The appearance of Lüders bands was noticed as a consequence of the interaction between niobium precipitates and dislocations during the subsequent cold deformation. In both variants of the industrial process performed on the cold deformed strip, Lüders bands appeared.

niobium microalloyed steel
thermomechanical processing
deformation
precipitation
dislocation density
microstructure

1. Materials and Methods

Low-carbon steel with a chemical composition of 0.12% C, 0.78% Mn, 0.18% Si, 0.020% Al, 0.0011% P, 0.018% S, and 0.0079% N microalloyed with 0.048% Nb was selected for this study. Two variants of industrial thermomechanical processing were implemented: high temperature (HT), in which the start of the final deformation occurred at 1020 Â°C, and low temperature (LT), in which the start of the final deformation occurred at 987 Â°C. The heating and austenitization were performed at 1250 Â°C for 3.1 h. The pre-deformation was carried out in the temperature range 1180â1040 Â°C with a total reduction of 92.25%.

Austenitizing and pre-deformation were completely identical in both variants. The degrees of deformation in all passes of the final deformation were also almost identical. In the LT variant, the final deformation was performed in the temperature range 987â887 Â°C, with five passes resulting in a total reduction of 83.10%. In the HT variant, the final deformation was also performed with five passes resulting in a total reduction of 82.98%, but in the temperature range 1020â905 Â°C. The strip was cooled to 560 Â°C and reeled. The temperature was measured using an optical pyrometer. A schematic of the final deformation is shown in Figure 1.

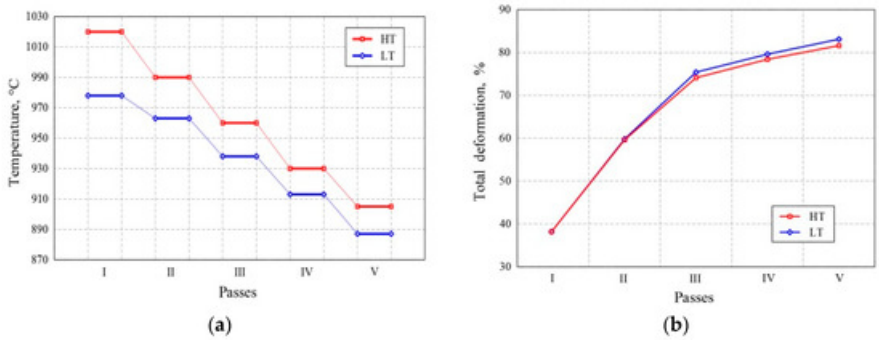

Figure 1. (**a**) Schematic of the final deformation (FD) and (**b**) the change in the degree of deformation.

Samples for testing were taken at characteristic spots from each phase of thermomechanical treatment. Sampling was carried out in such a way that the strip was stopped at a chosen moment. Then, the samples of interest from the deformation zone and its vicinity were rapidly cooled by applying the maximum amount of cooling water onto the rollers. In this way, the structural development and the processes involved in each phase of thermomechanical finishing were blocked. Reductions in the samples were determined using various methods of analysis. For electrochemical isolation, samples in the form of a plate with dimensions 80 mm Ã 20 mm were electrolytically dissolved in a cell according to the method described by W. Koch [1]. The isolate was identified using an atomic absorption spectrophotometer (AAS, Perkin Elmer, Waltham, MA, USA). The size and distribution of niobium precipitates, as well as their interaction with dislocations, were analyzed using a transmission electron microscope (TEM, JEOL-2000, Tokyo, Japan). For analysis by TEM, samples were prepared using the foil method. For that purpose, samples in the form of a cylinder with a diameter of 3 mm were used. They were mechanically ground on 600 and 1000 grit papers and then electrolytically thinned to a fully transparent foil. Electrolytical thinning was performed in a solution of 5% $HClO_4$ and 95% CH_3COOH using a voltage of 45 V at room temperature. The samples prepared in this way were analyzed using a transmission electron microscope at magnifications of 5000Ã and 200,000Ã and voltage of 200 kV. To determine the internal stresses in the material and the dislocation density, the X-ray diffraction method was used. Analyses were performed using a universal camera, a vertical diffractometer with BraggâBrentanoâs focusing, and a graphite monochromator using Co KÎ± radiation (Î» = 1.790 Ã). Samples with dimensions 10 mm Ã 10 mm were analyzed after metallographic preparation by grinding, polishing, and deep etching.

The microstructure of metallographically prepared samples after etching in nital was observed using a light microscope (Leitz Ortholux, Wetzlar, Germany), and images were taken using an Olympus digital camera. The appearance and propagation of the LÃ¼ders bands were analyzed by tensile testing, up to breaking point, on a Zwick 50 kN universal tensile testing machine (Zwick, Ulm, Germany). Simultaneous measurements of the temperature change in the deformation zone were taken using a VarioCAM M82910 thermographic camera (Jenoptik, Jena, Germany) with a temperature sensitivity of 80 mK. The measured results were analyzed using Irbis professional software (InfraTec GmbH, Dresden, Germany).

2. Results and Discussion

Figure 2 shows that in the pre-deformation in both variants, the degree of precipitation was low (11.8â12.1%) and did not change significantly from the onset to the end of pre-deformation. In the final deformation, there was an increase in the degree of precipitation in both variants. Nevertheless, it was slightly lower in the HT variant (25%) than in the LT variant (26%). The precipitation continued during the cooling phase of the strip and was higher for the high temperature variant (36.5%) as compared to low temperature variant (34%). Since in both

variants the steels were heated under the same conditions to the same temperature (1250 Â°C), it was assumed that the achieved solubility of niobium was the same in both variants.

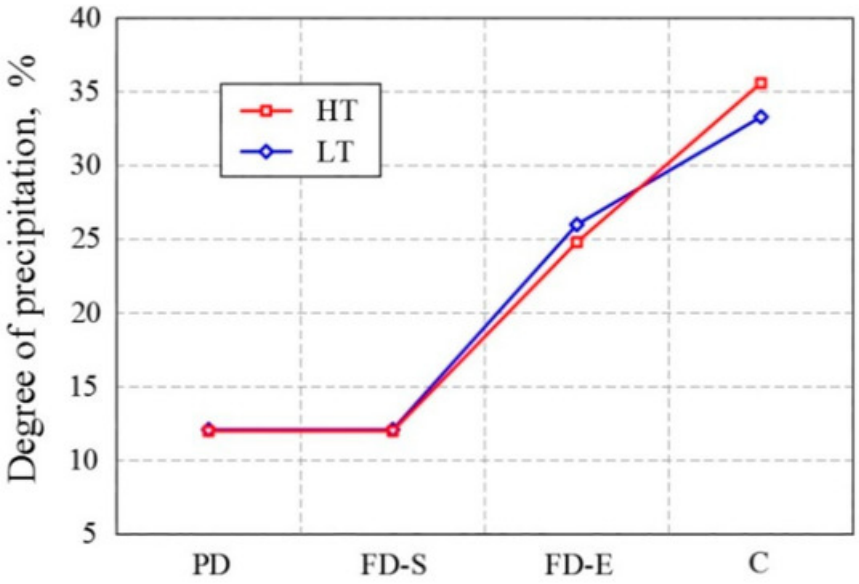

Figure 2. Degree of precipitation of niobium in each stage of thermomechanical processing. (PD: pre-deformation, FD-S: final deformationâstart, FD-E: final deformationâend, C: cooling).

Transmission electron analysis of the pre-deformed samples showed niobium precipitates (Figure 3). These precipitates were coarse, of spherical shape, and larger than 20 nanometers and were heterogeneously distributed in structure.

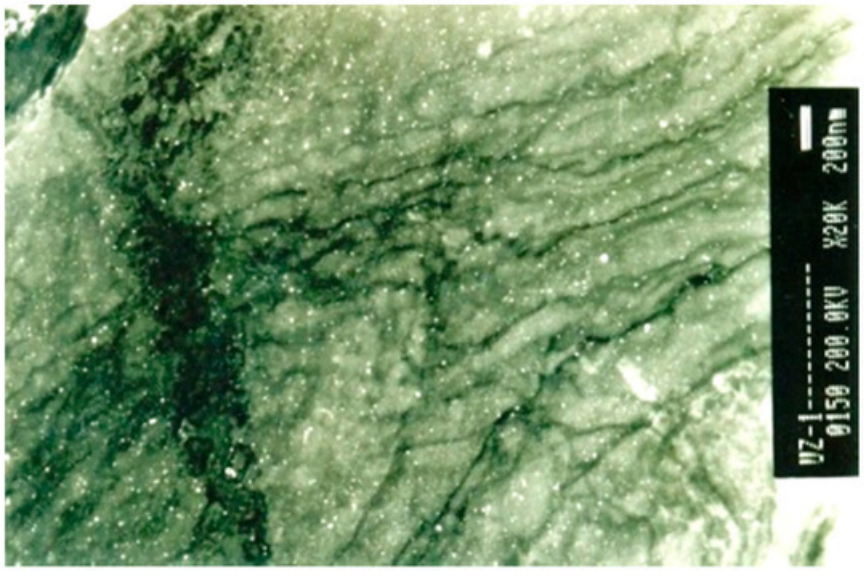

Figure 3. TEM micrograph of niobium precipitates in pre-deformation, reproduced from [2], with permission from Taylor&Francis, 2013.

In principle, precipitation of Nb carbides can occur in austenite or ferrite on grain boundaries, dislocations, subgrain boundaries, or interphase boundaries during the austenite-to-ferrite transformation [3].

In the final phase of thermomechanical treatment in both variants, the samples were examined after each pass (Figure 4a). The degree of precipitation in the HT variant was lower than that in the LT variant, and for the first three passes, they remained low and were similar for both variants (11.8â12.1%).

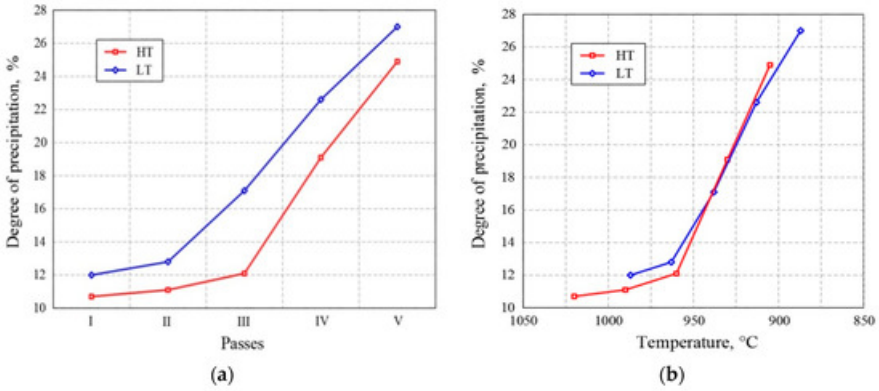

Figure 4. Change in precipitation degree (**a**) through passes and (**b**) with the temperature of thermomechanical processing.

Although it is known from the literature [4][5][6] that strain-induced precipitation is a function of temperature, deformation, and time, the results obtained in this study (shown in Figure 4) imply that SIP is more temperature dependent. In particular, in the low temperature variant, intensive, strain-induced precipitation started after the second pass (at 963 Â°C). In the high temperature variant, strain-induced precipitation began after the third pass (at 960 Â°C). Figure 4b clearly shows that the onset of intense strain-induced precipitation is more temperature dependent than the degree of deformation (Figure 4a). Strain-induced precipitation begins at a temperature of about 960 Â°C. It was found that, until the onset of strain-induced precipitation in both variants, dynamic and static recrystallization proceeded undisturbed. This is very important in the sense of the determination of hot rolling parameters. At 930 Â°C, the degree of precipitation was the same in both variants. In the fourth pass and in the fifth pass, there were significant increases in the degree of precipitation, amounting to 19% and 25%, respectively. Figure 4b clearly shows that with the decrease in temperature, the degree of precipitation increased in the LT as well as in the HT variant.

The beginning of strain-induced precipitation was also confirmed by transmission electron microanalysis (Figure 5). The strain-induced precipitates were very small, below 10 nanometers, and arranged in rows. The fraction of strain-induced precipitates and their average size are directly influenced by the amount of deformation [7].

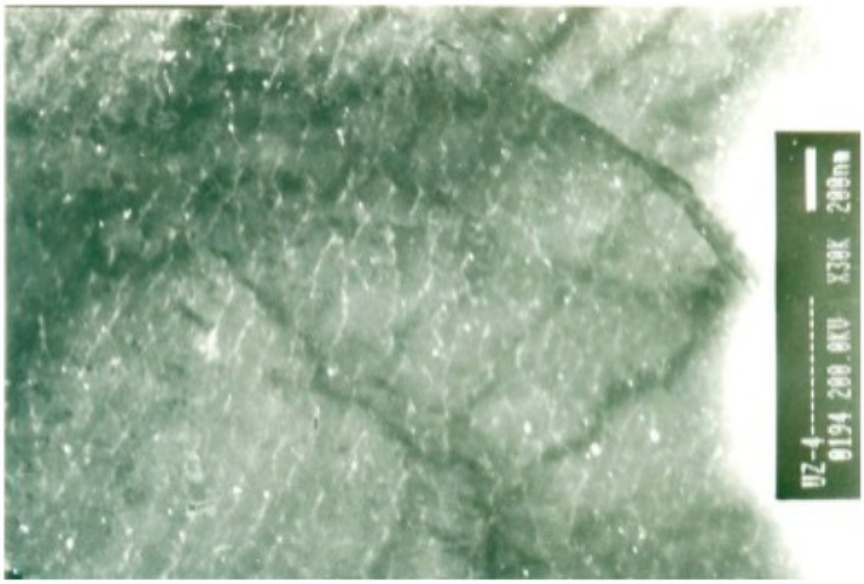

Figure 5. TEM micrograph showing the onset of strain-induced precipitation at 963 Â°C, low temperature (LT) variant.

In the last passes of the final thermomechanical processing in both variants, the degree of total

deformation decreases (Figure 6) while dislocation density increases, as is the case with the degree of precipitation (Figure 4a). In investigations of the same steels [8] it was proven that the low temperature rolling schedule leads to considerably higher rolling forces in the last three passes.

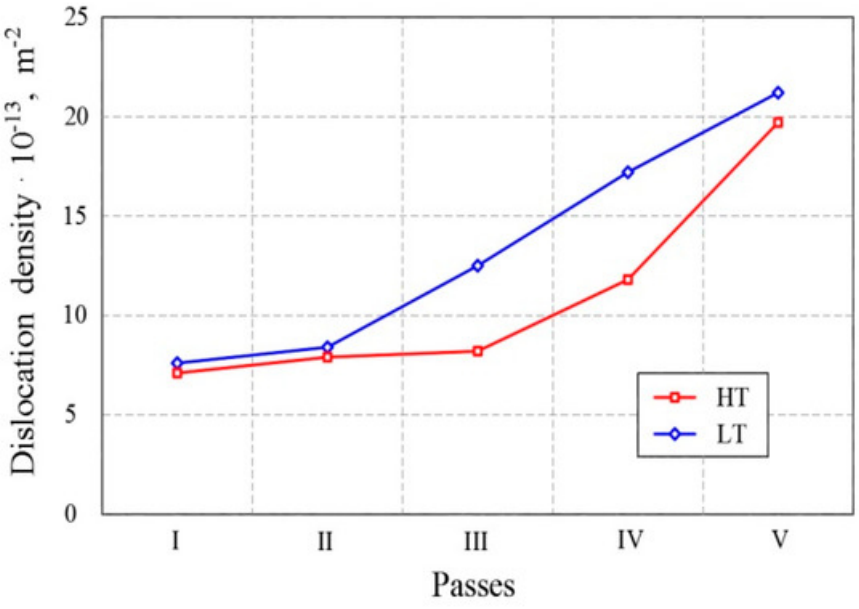

Figure 6. Change in the dislocation density by stages of final thermomechanical processing.

In order to determine the quantitative amount of changes in the structure, a study of the diffraction line profile was carried out. By studying the diffraction line profile in each pass of the HT and LT thermomechanical processing, a significant difference was observed both from the beginning to the end of the thermomechanical process and in each pass in both variants. From the profile of diffraction lines, the density of dislocations, Ï (mâ2), was calculated according to Equation (1).

The onset of strain-induced precipitation depended on the temperature, as is shown in Figure 7. In the first two passes, the degree of deformation was high and almost identical for both variants. Static and dynamic recrystallization took place undisturbed, so the dislocation density was lower. When strain-induced precipitation began at 960 Â°C, the recrystallization became inhibited and the dislocation density increased. In the last passes, the degree of deformation was small, but the density of dislocations increased as the degree of precipitation increased. Precipitates arranged in close-packed arrays became a strong obstacle to the movement of dislocations. Therefore, dislocations became immobile and their density increased.

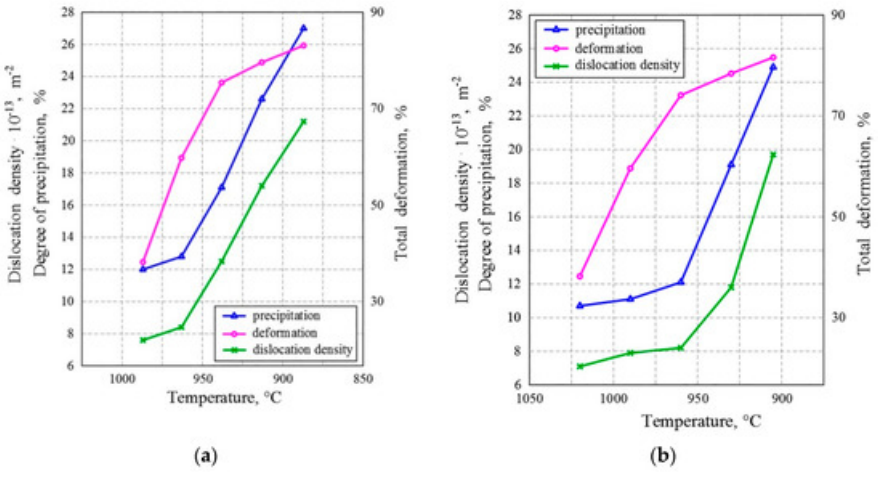

Figure 7. Relation between the degree of precipitation, the dislocation density, and temperature

for (**a**) the LT variant and (**b**) the HT variant.

Figure 7a shows that in the LT variant, the degree of precipitation almost linearly increased with the decrease in temperature after two passes. Dislocation density at the onset of deformation increased, but after the third pass, there was an evident slowdown, as can be seen in the values. Figure 7b shows similar tendencies for the HT variant, with the only difference being that a significant increase in the degree of precipitation and deformation occurred after the third pass. Further, it can be clearly seen that a change in the density of dislocations was associated with a change in the degree of precipitation. At the beginning of strain-induced precipitation, interaction of the precipitate and dislocations occurred and the dislocation density increased, as is shown in Figure 8.

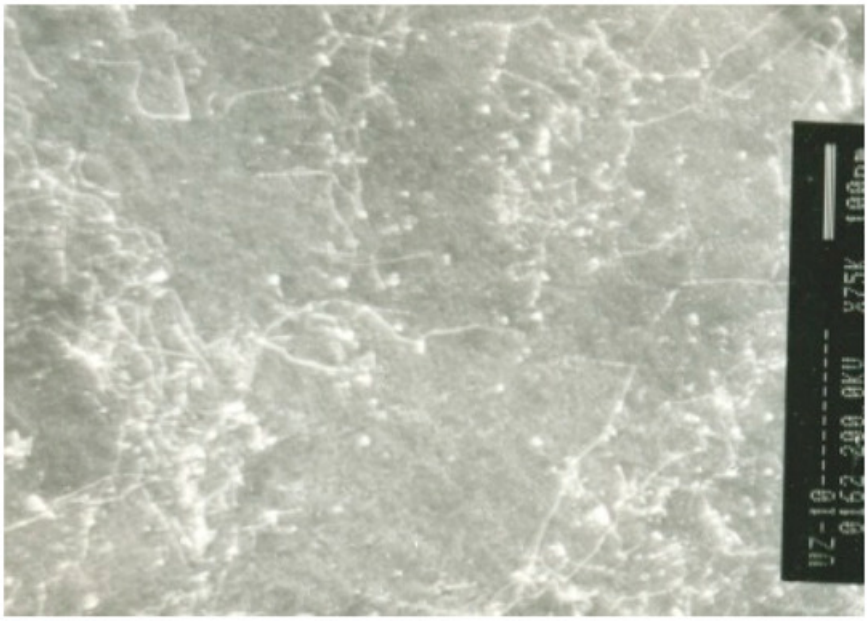

Figure 8. TEM micrograph of the interaction between precipitates and dislocations [9].

After the third pass, the major influence on the dislocation density was shown to be the degree of precipitation rather than the degree of deformation. Specifically, in microalloyed steels, recrystallization and precipitation can interact in at least three distinct ways [10]. Firstly, a decrease in dislocation density through recrystallization reduces the number of precipitate nucleation sites available and can thus retard the onset and rate of precipitation; this occurs after the onset of intense deformation-induced precipitation (960 Â°C) and is evident in the first two passes in the LT variant, as well as in the first three passes in the HT variant. Secondly, precipitate dispersion can provide a pinning (Zener) force that can retard or halt the progress of recrystallization; this is evident in the latest passes of final TMCP, because by increasing the degree of precipitation, the density of blocked dislocations also increases, as shown in Figure 7. Precipitates are arranged in rows at the onset of SIP (Figure 5), but after it, they are dispersed, accumulating in certain places and blocking the dislocations (Figure 8). Thirdly, the mobility of grain boundaries is strongly affected by the solute content of the matrix and its diffusivity. Particularly, the diffusivity of Nb is an important factor contributing to the significant retarding effect on recovery and recrystallization; it slows down boundary motion since it interacts with the boundary and does not diffuse rapidly enough to keep up with the migrating boundary. The higher degree of precipitation leads to the decrease in the amount of free Nb that can diffuse. Furthermore, as a result of the larger atomic radius of Nb than those of carbon, nitrogen, and iron, Nb moves more slowly; thus, it cannot track the grain boundary, and its diffusivity decreases. Further, the dislocation density increases even though the energy of the system and the temperature decrease, and so the total deformation slows down. Therefore, close-packed carbonitride rows and interaction between precipitates and dislocations are present in the

structure (Figure 9). The further increase in deformation and precipitation also increases the density of dislocations, as was also observed in [11]. Dislocations pile up on rows of precipitates and form the boundary of the subgrain (Figure 9).

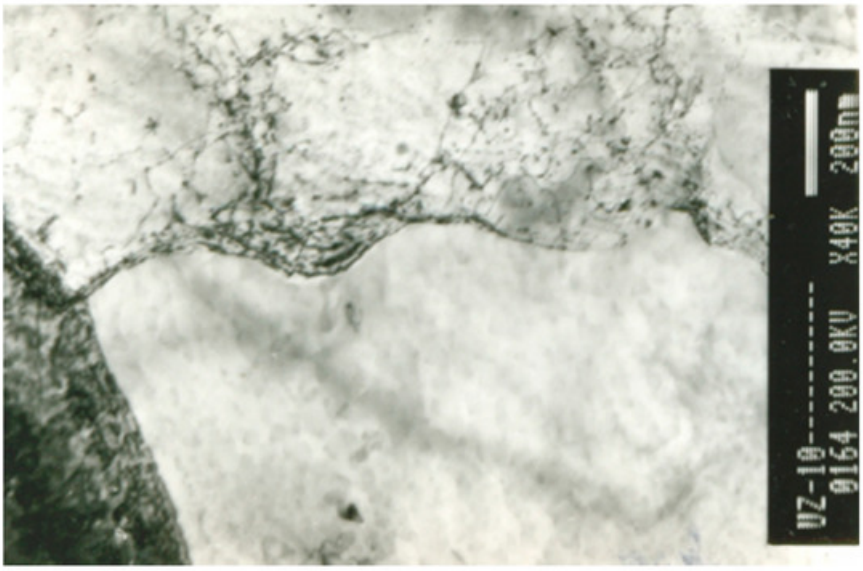

Figure 9. TEM micrograph of dislocations accumulating on the rows of precipitations.

In the last passes, the recrystallization and recovery mechanisms were halted and completely stopped. Specifically, fine precipitates pinned dislocations and thus retarded recovery. In such conditions, further deformation leads to an increase in the density of dislocations.

Before the phase transformation, there was enough solute niobium present in the steel to delay the transformation. Specifically, solute niobium delays transformation significantly, which lowers the temperature, resulting in a higher ferrite nucleation rate and lower ferrite growth rate. As the phase transformation takes place relatively slowly, there is a possibility for interphase precipitation. After slow cooling, which occurs in the air, there is a chance for spontaneous precipitation [12]. In this study, it was found that in the HT variant, precipitation of 36.5% was achieved, and in the LT variant, 34% was achieved. As a final step of TMCP, after rolling, both strips (the LT and HT variants) were cooled at the same speed. Precipitation continued, and these precipitates had a beneficial effect in preventing ferritic perlite grain growth. A fine-grained, ferriteâpearlite microstructure with almost the same grain size was achieved (Figure 10).

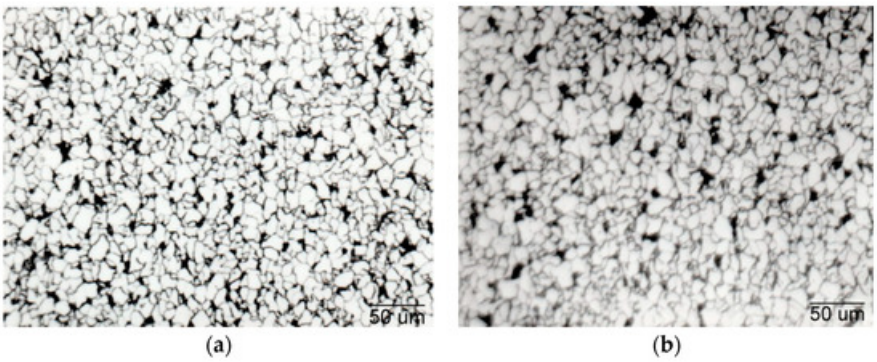

Figure 10. Microstructure of the hot rolled strips of Nb microalloyed steel. (**a**) LT variant. (**b**) HT variant.

In both variants of TMCP, the precipitation of Nb, the interaction of precipitates, and dislocations resulted in a fine-grained, homogeneous structure. In the cooled strip, the degree of precipitation in the high temperature variant (36.5%) was higher as compared to that in the low temperature variant (34%). This indicates that the binding of niobium to precipitates (NbC, NbN, Nb(CN)) was

not accomplished entirely. Free niobium may affect the appearance of LÃ¼ders bands. The dislocation density was about the same, 10^8 $m^{â2}$. Steels of similar chemical composition but not containing Nb have a dislocation density of 10^6 $m^{â2}$.

The subsequent cold deformation of the strip shows the appearance of inhomogeneous deformations at the beginning of the plastic flow of the material. These inhomogeneous deformations (stressâstrain curve) are related to the appearance of LÃ¼ders bands (Figure 10). Specifically, LÃ¼ders bands are localized regions of plastic deformation that are often observed in cold-rolled low-carbon steel following the appearance after the limit of proportionality[13][14][15][16][17][18].

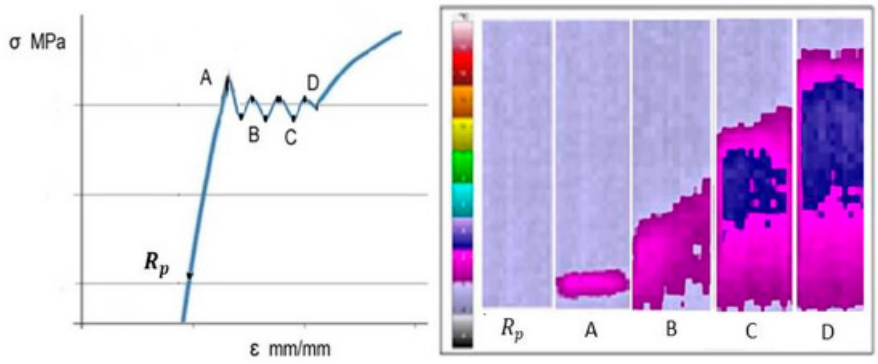

Figure 11. The stressâstrain curve and distribution of temperature change at the beginning of the plastic material flow in the field of the appearance of LÃ¼ders bands.

When the interaction energy between dislocations and easily diffused solute atoms (C, N, and Nb) is strong, they gather around dislocations to form Cottrellâs atmospheres. Then, dislocations are strongly anchored and the stored energy of the dislocation is decreased. When the upper yield point is reached in cold deformation, the number of moving dislocations increases because of the formation of new dislocations as a result of the multiplication mechanism. Moving dislocations are formed only at the places of the highest stress concentration. This moment corresponds to the development of LÃ¼ders bands. The appearance of LÃ¼ders bands was observed in both variants [13] as a consequence of the interaction between niobium strain-induced precipitates and dislocations during cold deformation [15].

3. Conclusions

Research conducted within the framework of this paper resulted in the following conclusions:

- During the final thermomechanical processing of niobium microalloyed steel, the onset of deformation-induced precipitation begins at 960â963 Â°C. Precipitation is continuous during the final deformation phase and during the cooling period. At the end, a significant amount of free niobium remained in both variants;
- The increase in the density of dislocations before the onset of intense precipitation is insignificant because in the material, in addition to deformation, recrystallization and recovery occur;
- With the onset of strain-induced precipitation, the density of dislocations increases. This indicates that the recrystallization and recovery mechanisms are slowing down or are completely absent, with further deformation and precipitation being caused by the niobium content. As the degree of niobium strain-induced precipitation increases, the density of dislocations also increases.

Finally, niobium precipitates determine the density of dislocations. The interaction of niobium precipitations and dislocations, as well as free niobium, carbon, and nitrogen, could be related to

the inhomogeneous deformations that are associated with the appearance of LÃ¼ders bands.

References

1. Koch, W. Electrolytic Isolation of Carbide in Alloyed and Unalloyed Steels; Stahl, U.E., 69(1); 1949; p. 69.
2. F. Vodopivec; S. Src=; Evolution of substructure during continuous rolling of microalloyed steel strip. , , , 10.1179/026708399101505248.
3. M. Charleux; W. J. Poole; M. Militzer; A. Deschamps; Precipitation behavior and its effect on strengthening of an HSLA-Nb/Ti steel. *Metallurgical and Materials Transactions A* **2001**, *32*, 1635-1647, 10.1007/s11661-001-0142-6.
4. Najafi-Zadeh, A.; Yue, S.; Jonas, J.J. Influence of hot strip rolling parameters on austenite recrystallization in interstitial free steels. ISIJ Int. 1992, 32, 213â221.
5. Taku Sakai; Andrey Belyakov; Rustam Kaibyshev; Hiromi Miura; John J. Jonas; Dynamic and post-dynamic recrystallization under hot, cold and severe plastic deformation conditions. *Progress in Materials Science* **2014**, *60*, 130-207, 10.1016/j.pmatsci.2013.09.002.
6. I. Weiss; J. J. Jonas; Interaction between recrystallization and precipitation during the high temperature deformation of HSLA steels. *Metallurgical and Materials Transactions A* **1979**, *10*, 831-840, 10.1007/bf02658301.
7. Roxana Hutanu; Lynann Clapham; R.B. Rogge; Intergranular strain and texture in steel Luders bands. *Acta Materialia* **2005**, *53*, 3517-3524, 10.1016/j.actamat.2005.04.008.
8. F. Vodopivec; S. Src=; Evolution of substructure during continuous rolling of microalloyed steel strip. , , , 10.1179/026708399101505248.
9. Stoja ReÅ¡koviÄ; Ivan JandrliÄ; Influence of Niobium on the Beginning of the Plastic Flow of Material during Cold Deformation. *The Scientific World Journal* **2013**, *2013*, 1-5, 10.1155/2013/723725.
10. Vervynckt, S.; Verbeken, K.; Lopez, B.; Jonas, J.J. Modern HSLA steels and role of non-recrystallisation temperature. Int. Mater. Rev. 2012, 57, 187â207.
11. ReÅ¡koviÄ, S.; Vodopivec, F.; Novosel-RadoviÄ, V.; MamuziÄ, I. The influence of a hot plastic deformation on the crystal latice distortion change of a thermomechanical treatment microalloyed steel. In Proceedings of the 5th International Scientific Conference on Production Engineering CIM â99, Opatija, Croatia, 17â18 June 1999; Croatian Association of Production Engineering: Zagreb, Croatia, 1999; pp. 121â129.
12. Tao Jia; Matthias Militzer; The Effect of Solute Nb on the Austenite-to-Ferrite Transformation. *Metallurgical and Materials Transactions A* **2014**, *46*, 614-621, 10.1007/s11661-014-2659-5.
13. F. Garofalo; Factors affecting the propagation of a lÃ¼derâs band and the lower yield and flow stresses in iron. *Metallurgical and Materials Transactions A* **1971**, *2*, 2315-2317, 10.1007/bf02917580.
14. Petit, J.; Wagner, D.; Ranc, N.; Montay, G.; Francois, M. Comparison of different techniques for the monitoring of the LÃ¼ders bands development. In Proceedings of the International Congress on Fracture, Bejing, China, 26â30 May 2013.
15. Stoja ReÅ¡koviÄ; BrliÄ Tin; JandrliÄ Ivan; Vodopivec Franc; Influence of Strip Cooling Rate on LÃ¼ders Bands Appearance During Subsequent Cold Deformation. *Mathematical Methods and Modelling in Applied Sciences* **2019**, , 115-121, 10.1007/978-3-030-18072-0_12.
16. Stoja ReÅ¡koviÄ; I JandrliÄ; Tin BrliÄ; The influence of niobium content and initial microstructure

of steel on the occurrence of LÃ¼ders band at the start of the plastic flow during cold deformation. *IOP Conference Series: Materials Science and Engineering* **2018**, *461*, 012070, 10.1088/1757-899x/461/1/012070.

17. Tin BrliÄ; Stoja ReÅ¡koviÄ; I JandrliÄ; F Skender; Influence of strain rate on stress changes during LÃ¼ders bands formation and propagation. *IOP Conference Series: Materials Science and Engineering* **2018**, *461*, 012007, 10.1088/1757-899x/461/1/012007.
18. Ivan JandrliÄ; Stoja ReÅ¡koviÄ; Tin BrliÄ; Distribution of Stress in Deformation Zone of Niobium Microalloyed Steel. *Metals and Materials International* **2018**, *24*, 746-751, 10.1007/s12540-018-0099-2.
